Soft Matter

Accepted Manuscript

ROYAL SOCIETY OF CHEMISTRY

www.rsc.org/softmatter

Self-healing Multilayer Polyelectrolyte Composite Film with Chitosan and Poly (acrylic acid)

Yanxi Zhu[a], Hongyun Xuan[a], Jiaoyu Ren[a], Liqin Ge[a1]

[a]State Key Laboratory of Bioelectronics, School of Biological Science and Medical Engineering, Southeast University, Nanjing 210096, P. R. China

Abstract: If self-healing materials can be prepared via simple technology and methods using nontoxic materials, this would be a great step forward in the creation of environmentally friendly self-healing materials. In this paper, the specific structural parameters of the various hydrogen bonds between chitosan (CS) and polyacrylic acid (PAA) were calculated. Then, multilayer polyelectrolyte films were fabricated with CS and PAA based on layer-by-layer (LbL) self-assemble technology at different pH values. The possible influence of pH on the (CS/PAA)*30 multilayer polyelectrolyte film were investigated. The results show that the interactions between CS and PAA, swelling capacity, microstructure, wettability, and self-healing ability are all governed by the pH of the CS solution. When the pH value of the CS solution is 3.0, the prepared multilayer polyelectrolyte film (CS3.0/PAA2.8)*30 has fine-tuned interactions, a network-like structure, good swelling ability, good hydrophilicity, and excellent self-healing ability. This promises to greatly widen the future applications of environmentally friendly materials and bio-materials.

Keywords: CS; PAA; LbL; Self-healing; pH

1. Introduction

Human skin, which can heal itself after impaired, offers a good inspiration to study and design self-healing materials with enhanced properties of safety and durability, leading to their long-term use with stable functionality. Based on the healing mechanisms, self-healing materials can be grouped into extrinsic self-healing materials and intrinsic self-healing materials.[1] Extrinsic self-healing materials,

[1]Corresponding author at: State Key Laboratory of Bioelectronics, Biological Science and Medical Engineering Department, Southeast University, Nanjing 210096, PR China. Tel.: +86 2583619983; fax: +86 2583795635.
E-mail address: lqge@seu.edu.cn.

including capsule-based healing systems[2] and vascular healing systems, complete their self-healing process via releasing healing agents after crack propagation;[3] while intrinsic self-healing materials based on either covalent interactions,[4-6] such as Diels–Alder (DA) and retro Diels–Alder (RDA) processes,[7] or non-covalent interactions[8] such as hydrogen bonds,[9-11] ionic interactions,[12] π-π interactions,[13] host-guest interactions,[14] metal-ligand coordination,[15] and supramolecular interactions.[16]

The preparation processes of extrinsic self-healing materials and intrinsic self-healing materials are both complicated and difficult in reported literatures.[17, 18] Moreover, organic solvent or toxic raw materials are essential to synthesis processes, causing the obvious toxic side effects of the self-healing materials,[19, 20] which limit the application of the self-healing materials in some extent. With the continuous development of human civilization process, environment-friendly materials, designed by green preparation technique and stock, have become all the more important. If the self-healing materials can be prepared via simple and green technology by nontoxic materials with properties of excellent biocompatibility, the developed progress of environment-friendly self-healing materials will be greatly promoted.

In the past decades, LbL self-assembly technique has attracted more and more attentions because the widely used thin films can be conveniently prepared by this method. LbL self-assembly technique was also used for the formation of stimuli responsive self-healing films, for LbL self-assembly technique is typically accomplished by alternating the adsorption of mutually interacting polymers on surfaces, is adjustable to different classes of low and high molecular weight compounds; more importantly, LbL self-assembly technique can be driven by multiple weak interactions, including electrostatic interactions, hydrogen-bonds, halogen-bonds, coordination bonds, charge-transfer interactions, guest–host interactions, cation–dipole interactions, and the combined interactions of the above forces,[21] which are often employed to design of self-healing materials. Thus, LbL self-assembly technique is a versatile and easy approach to design nanostructure thin films with self-healing ability. Recently, there are many achievements in development, formation and application of “smart” self-healing materials prepared via LbL

self-assembly techniques.[22-28] In our previous work, bioinspired self-healing film with good electrochemical performance was also prepared based on LbL self-assembly technique.[29]

CS is a typical copolymer of D-glucosamine and N-acetylglucosamine derived from chitin. CS has attracted enthusiastic attention due to its renewability, biodegradability, bacteriostatic and biocompatibility, it has potential applications ranged from biomedicine and pharmacy to water treatment.[30, 31] Furthermore, CS has multiple amino groups, which can be protonized in acid aqueous solution and can form composites with negatively charged molecules or materials, thus is often be used to fabricate novel thin films and microcapsules by LbL self-assemble technology. PAA is nontoxic and negatively charged after dissolved in water.[32, 33] PAA has carboxyl in its monomer, which can react with amino in CS and generate supramolecular copolymer with structure of hydrogen bond. It is a promising candidate to synthesize self-healing materials with CS through LbL self-assemble technology.

In this paper, self-healing multilayer polyelectrolyte film, (CSn/PAA2.8)*30 (n=4.0, 3.5 and 3.0, n represent the pH of CS solution, 2.8 represent the pH of PAA solution), were fabricated with green stock, CS and PAA, based on green technology, LbL self-assemble technology, at different pH values, and the preparation mechanism, compositions, microstructures, wettability, self-healing properties and electrochemical properties of the (CSn/PAA2.8)*30 multilayer polyelectrolyte films were investigated. The results show that the (CS3.0/PAA2.8)*30 self-healing multilayer polyelectrolyte film has fine-tuned interactions, network-like structure, good swelling ability, super-hydrophilicity and excellent self-healing ability in water environment. It is promised to be greatly broaden the future application in bio-materials.

2. Experimental

2.1. Chemicals and materials

Ethanol and acetic acid were obtained from Sinopharm Chemical Reagent Shanghai Co. Ltd. PAA (Mw≈18000) and CS (Mw≈375000, The degree of N-deacetylation (DD) is 85%) were obtained from Sigma-Aldrich Co. Ltd. All other reagents were used as

received. The concentrations of aqueous polyelectrolyte solutions used for film fabrication was 4 mg mL^{-1}, the pH value of PAA was 2.8, while the pH value of CS is ranged from 2.5 to 4.0, and the pH was adjusted with either 1 M acetic acid or 1 M NaOH. The glass substrate was soaked in the mixture of 98% H_2SO_4/30% H_2O_2 (volumetric ratio 3:1) for 24 h. Then the glass substrate was rinsed with ethyl alcohol and ultrapure water several times, and finally it was dried with N2 stream. And the obtained glass substrates was negatively charged after the treatment.

2.2. The synthetic process of the self-healing multilayer polyelectrolyte films.

The schematic diagram of the multilayer polyelectrolyte films' ((CSn/PAA2.8)*30) synthetic process is shown in Fig. 1. First, the prepared glass was immersed in CS solution for 15 min; then, the substrate was soaked in ultrapure water for 5 min to remove the CS that didn't adsorb on substrate. Second, to obtain (CSn/PAA2.8) *1, the CS-substrate was immersed in PAA solution for 15 min, then the (CSn/PAA2.8) *1 was soaked in ultrapure water for 5 min to remove the PAA that didn't adsorb on CS-substrate. Repeated first and second processes 29 times, the (CSn/PAA2.8)*30 was obtained.

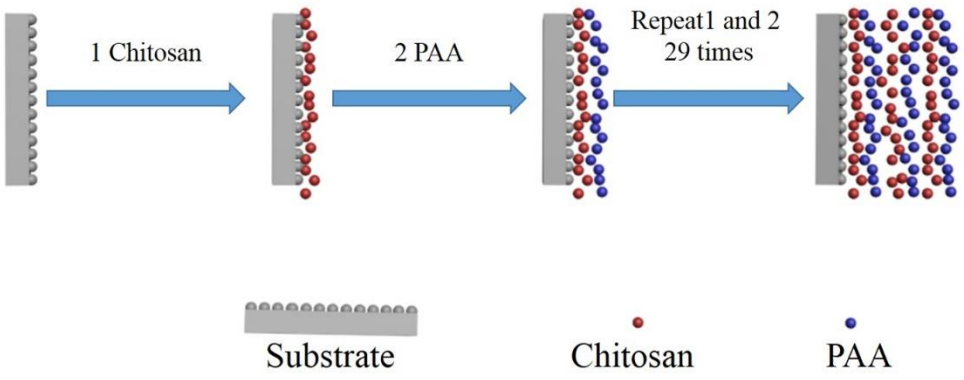

Fig. 1 The schematic diagram of the multilayer polyelectrolyte films' synthetic process ((CSn/PAA2.8)*30 (n=4.0, 3.5 and 3.0 respectively)).

2.4 Characterization

FT-IR spectrum of the prepared samples was obtained on Nicolet 5700 (Thermo Electron Scientific Instruments Corp). The surface morphologys of the prepared samples was characterized by field emission scanning electron microscopy (FESEM,

Ultra Plus Zeiss). The water contact angle of the prepared samples was analyzed using inductively coupled plasma atomic emission spectroscopy (ICP-AES, Shanghai Zhongchen Digital Technology Equipment Co., Ltd., Shanghai, China). The self-healing process of the samples was observed by Stereo Microscope (MVX10 OLYMPUS). Electrochemical impedance spectroscopy (EIS) measurement was carried out using the electrochemical workstation (chi660d CHI instruments Inc., Shanghai, P. R China) at open circuit potential with a superimposed 5 mV sinusoidal voltage in the frequency range from 10^4 Hz to 10^{-2} Hz. The prepared self-healing multilayer polyelectrolyte films were used as working electrode. The counter electrode was a piece of platinum sheet and the reference electrode was an Ag/AgCl electrode. A 2 mM $K_3Fe(CN)_6$ phosphate buffer saline (PBS, pH 7.0) solution was used as electrolyte.

3 Results and discussions

The Accelrys Discovery Studio 2.1 (DS 2.1) software program is usually used to identify the hydrogen bonds, as well as the hydrophobic, hydrophilic, electrostatic, and coordination interactions, of compounds.[34,35] In this paper, using the density functional theory (DFT) model of the Gaussian09[36] program, the geometrical structures of the PAA molecule were fully optimized by employing the B3LYP[37] method. Then, DS 2.1 was used to simulate the formation process of CS/PAA film. The CS molecule was defined as the acceptor, and the PAA molecule was defined as the ligand. After docking with ZDOCK modules, [38] the optimal configuration (Fig. 2) was selected from the obtained results based on the principle of energy minimization. We used ChemDraw Ultra7.0 software to draw a schematic diagram of the 2D hydrogen-bond interactions between CS and PAA according to the 3D interactions shown in Fig.2. From Fig. 2 and Scheme 1, we find that PAA and CS can form strong hydrogen bonds in theory and that no other interactions between them exist, so they are very suitable for designing self-healing materials. The specific structural parameters of the various hydrogen bonds are shown in Table 1. As can be seen from Table 1, the H_{80} in CS and the O_{32} in PAA can form a strong hydrogen bond; the H_{30}

on the carboxyl in PAA can form a strong hydrogen bond with the O_{20} in CS. The H that connects with the O_7 in CS can form hydrogen bond with the O_{37} in PAA. Also, the interactions between them were calculated as -141 kcal/mol. The reason CS can form these strong interactions with the PAA molecule may relate to the following factors: firstly, CS has a flexible and strong structure that can easily deform and reform into a spatial matching configuration. Also, there are abundant amino and hydroxyl groups in CS, and PAA molecules contains many carboxyl groups. Thus, they can react with one another easily and generate a supramolecular copolymer.

In intrinsically self-healing materials, the non-covalent interactions can usually be dynamically associated or dissociated with certain stimuli. Although the interactions between CS and PAA take place via hydrogen bonding, which is commonly used to design self-healing materials, it cannot dynamically associate/dissociate with water stimulation, so it is necessary to change the bond length and bond angle of the hydrogen bond to achieve the goal of self-healing. Many articles[39,40] have reported that the charges in weak polyelectrolytes can be gradually switched on or off by changing the pH of the environment. By controlling the pH, the charge density along the polymer backbone can be varied, and thus, the strength of the interactions with the neighboring counter-polyion can be fine-tuned.[27] Therefore, environmentally friendly self-healing materials can very likely be fabricated with non-toxic CS and PAA through LbL self-assembling technology simply by controlling the pH during the synthesis process.

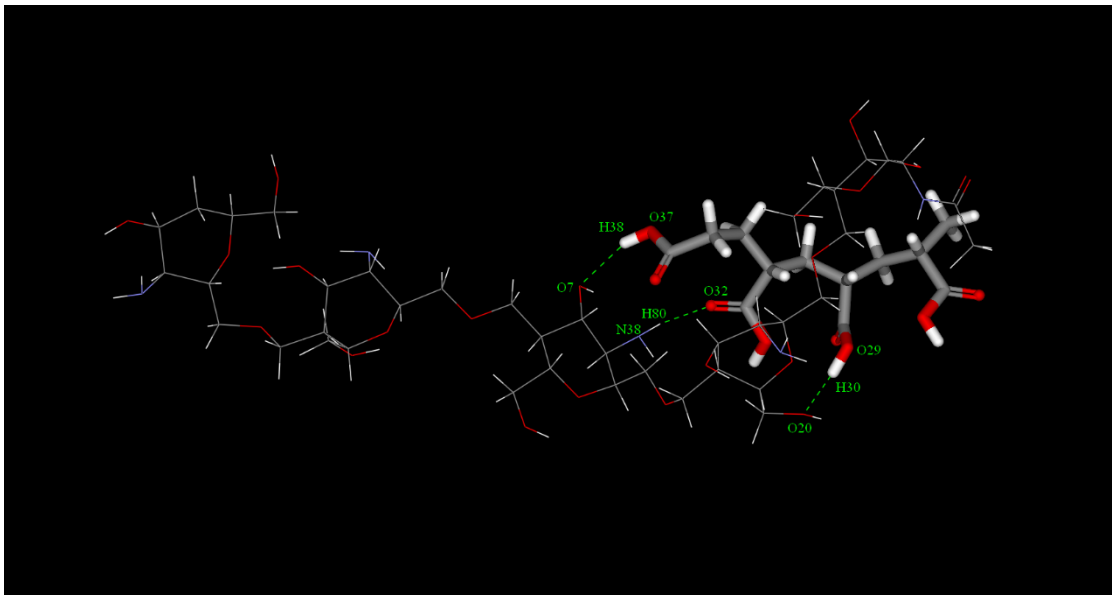

Fig. 2 Configuration schematic of interactions between CS and PAA, Hydrogen bonds are shown with green dashed lines. (Image obtained with Accelrys DS Visualiser software).

Table 1 The parameter list of CS and PAA（D:CS; A：PAA）

Bond position	$d_{(D-H)}$ (Å)	$d_{(H\cdots A)}$ (Å)	$d_{(D\cdots A)}$ (Å)	∠DHA (°)
A: N_{38}–H_{80} ··O_{32}: D	1.03	1.85	2.81	154.2
D: O_{29}–H_{30} ··O_{20}: A	0.95	2.00	2.84	145.7
D: O_{37} ··H_{38}–O_7: A	0.95	2.39	3.28	154.9

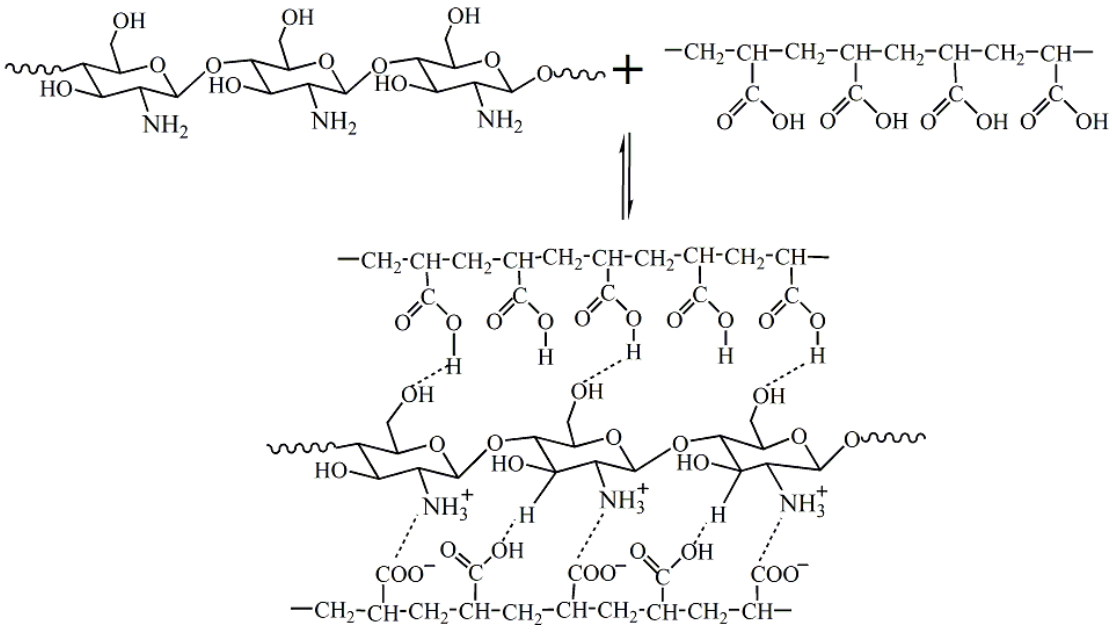

Scheme 1. Schematic illustration of the 2D hydrogen-bond interactions between CS and PAA.

The FT-IR spectra of polyelectrolyte composite films prepared from CS and PAA at different pH values (when the pH value is 2.5, the sample was equal volumes of CS and PAA mixed solution) are given in Fig.3. To investigate the changes in the chemical bond, the FT-IR spectra of pure CS and PAA are also given. The characteristic peaks of pure CS appeared at 3,400 cm^{-1} for the hydroxyl group and 1,650 and 1,590 cm^{-1} for the amide I and II groups, while in the spectrum of pure PAA, characteristic peaks at 3,410, 1,730 and 1,459 cm^{-1} can be clearly observed. In the sample of (CS4.0/PAA2.8)*30, many distinct new peaks appeared. The peak that appeared at 1,554 cm^{-1} confirmed the presence of $-NH^{3+}$ in (CS4.0/PAA2.8)*30 films,[41] and the peak at 1,643 cm^{-1} confirms the presence of an $-NH^{2+}-$ group in (CS4.0/PAA2.8)*30 films. Furthermore, the absorption peaks at 1,414 cm^{-1} can be assigned to the asymmetric and symmetric stretching vibrations of the carboxyl group.[42] These movements of peaks all prove that CS and PAA can react with one another[43] and form strong hydrogen bonds at a high pH. In the samples of (CS3.5/PAA2.8)*30 and (CS3.0/PAA2.8)*30, the new peak for symmetric$-NH^{3+}$ at 1,554cm^{-1} slowly shift to 1,538 cm^{-1}, and the peak at 1,643 cm^{-1} shifted to 1,623 cm^{-1}. This is because the concentration of H^{+} in the CS solution increases as the pH changes from 4.0 to 3.0, increasing to the protonation degree of the CS and decreasing the bond energy of the hydrogen bond between CS and PAA. This results in reduced interactions between PAA and CS. When the pH is 2.5, the protonation degree of CS is too strong to react with PAA to generate a copolymer with hydrogen bonds. The obtained result suggests that the interactions between PAA and CS weakened as the pH decreased, which is consistent with the above speculation in Fig.2. The results indicate that the fine-tuned hydrogen bond can associate/dissociate via stimulation, which is a decisive factor in the self-healing abilities of (CSn/PAA2.8)*30 composites films and is governed by the pH of the CS solutions.

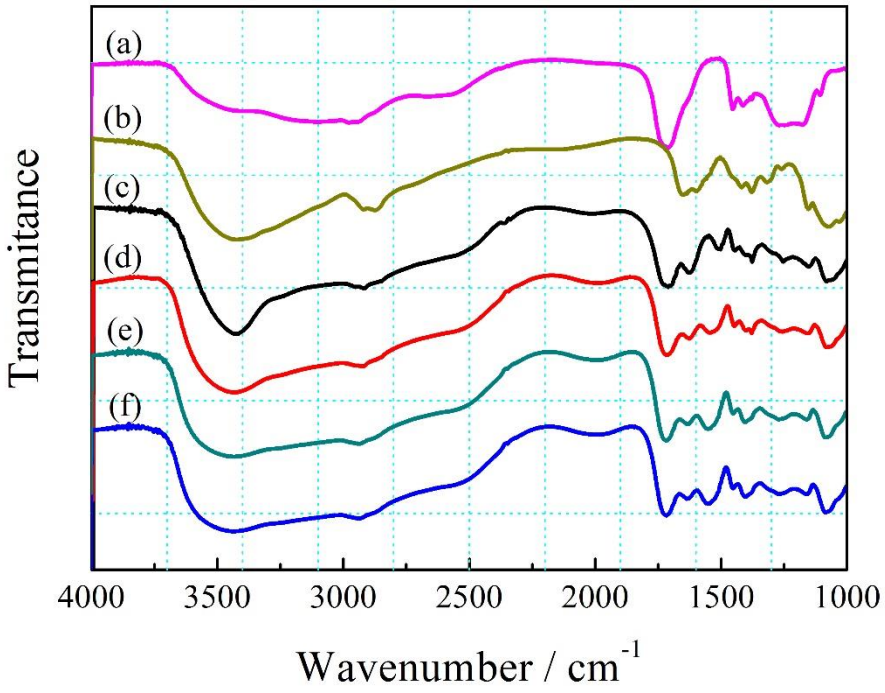

Fig. 3 FT-IR spectra of a) PAA powder, b) CS powder, c) PAA and CS (pH value of CS solution is 2.5) mixture, d) (CS3.0/PAA2.8)*30, e) (CS3.5/PAA2.8)*30 and f) (CS4.0/PAA2.8)*30 multilayer polyelectrolyte films.

Because the prepared samples engage in the self-healing process in water, it is essential to study the structural changes that occur between the dried state and the hydrated state. When the sample is dried at room temperature, it will collapse because of the surface tension and lose its structure. While the freeze-drying technique is based on dehydration via the sublimation of a frozen product, due to the absence of liquid water and the low temperatures required for the process, it can maximize the maintenance of the sample's real structure in the hydrated state. We employed a freeze-drying technique to maintain the sample's real structure and observed it using FESEM. Images (a), (b), and (c) all present a smooth surface, and there is little difference among them when they are dried at room temperature. However, their freeze-dried images differ dramatically. As shown in (d)-(f), the (CS4.0/PAA2.8)*30 film (d) presents a flat and smooth surface as shown in (a); the freeze-dried-state (CS3.5/PAA2.8)*30 film (e) clearly shows a difference with the film in (b) in that it is composed of hundreds of fragments, while the (CS3.0/PAA2.8)*30 film (f) has an

integrated surface that is composed of a highly-porous and network-like structure. It is obviously different than the one in (c). This is because with the pH decreasing, the multilayer polyelectrolyte film swells, which will result in a loosened structure; also, the different interactions between CS and PAA under different conditions causes different surface roughness.

In contrast to images (a), (b), and (c), images (g), (h), and (i) display many differences, the most obvious being that as pH decreased, the condensed structures become slightly loosened and their thickness also changes, ranging from 30 to 60 μm. Comparing cross-sectional images of (g) with (j), (h) with (k), and (i) with (l), we find that (g) and (j) show little difference, while the thicknesses of (k) and (l) are above 300 μm, at least five times those of (h) and (i). These changes further proved that at a high pH, (CSn/PAA2.8)*30 multilayer polyelectrolyte films do not exert enough repulsive force on hydrogel swelling,[43] resulting in a decreased swelling ability.[44] The results indicate that the expandability and the microstructure of the as-prepared (CSn/PAA2.8)*30 composite films, which are the key factors in its self-healing abilities, are also governed by the pH of the CS solutions.

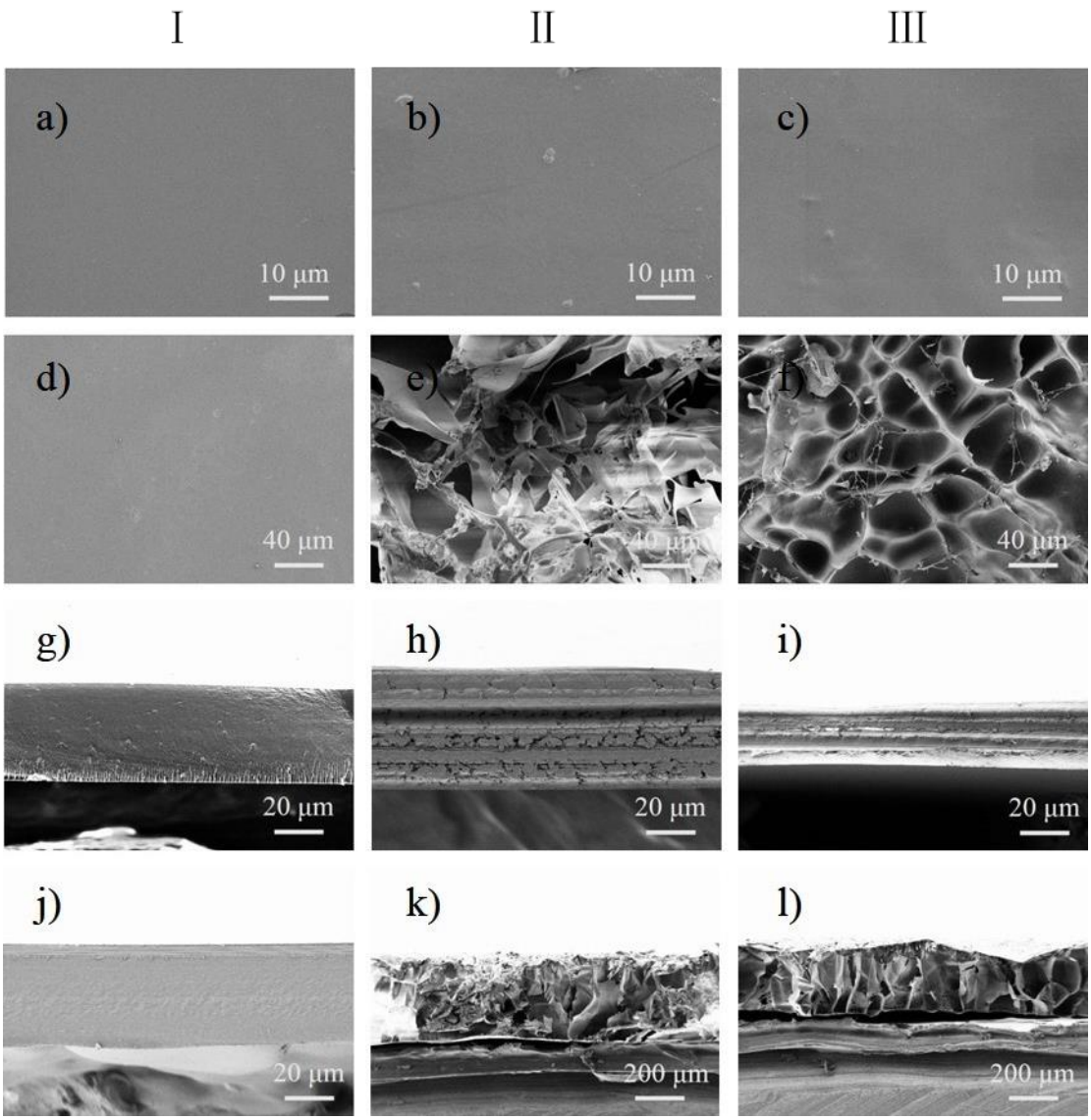

Fig. 4 FESEM images of I) (CS4.0/PAA2.8)*30 (a, d, g, j); II) (CS3.5/PAA2.8)*30 (b, e, h, k); III) (CS3.0/PAA2.8)*30 (c, f, i, l) multilayer polyelectrolyte films. (a-c) show the surface structure and the (g-i) show the cross-sectional structure of the film which is dried at room temperature; (d-f) show the surface structure and the (j-l) show the cross-sectional structure of the film which is treated with the freeze-dried technique.

When the prepared self-healing multilayer polyelectrolyte films is going through the self-healing process, the initiator (water) can diffuse and infiltrate a hydrophilic surface more quickly and easily than one in a hydrophobic surface, which will result in the hydrophilic multilayer polyelectrolyte film repairing itself. In theory, all other factors being equal, the smaller the water contact angle of the self-healing multilayer

polyelectrolyte films, the more readily the self-healing multilayer polyelectrolyte films will engage in the self-healing process, so the wettability of the self-healing multilayer polyelectrolyte surfaces can be determined as part of the self-healing design.[45] Thus, we investigated the wettability of (CSn/PAA2.8)*30 multilayer polyelectrolyte films prepared at various pH values by measuring their water contact angle, and the figures are given in Fig. 5. From the given figures, we can find that the water contact angle of (CS4.0/PAA2.8)*30 multilayer polyelectrolyte film is 74.3 °. The water contact angle of (CS3.5/PAA2.8)*30 multilayer polyelectrolyte film changes to 56.7 °, while the water contact angle of (CS3.0/PAA2.8)*30 is 27.1 °, indicating that (CS3.0/PAA2.8)*30 multilayer polyelectrolyte film is a more hydrophilic film. This is because CS exhibits pH-responsive behavior as a weak polyelectrolyte due to the large quantities of amino groups in its backbone; in a low-pH solution, the protonation of the $–NH^{2+}$ group in the multilayer polyelectrolyte film thus ensures chain relaxation, which is advantageous in terms of efficient solvent diffusion. The multilayer film surface will become more hydrophilic.[46] From the water contact angle results above, one can conclude that the wettability of the as-prepared (CSn/PAA2.8)*30 composite films, another major factor in self-healing ability, is also governed by the pH of the CS solutions.

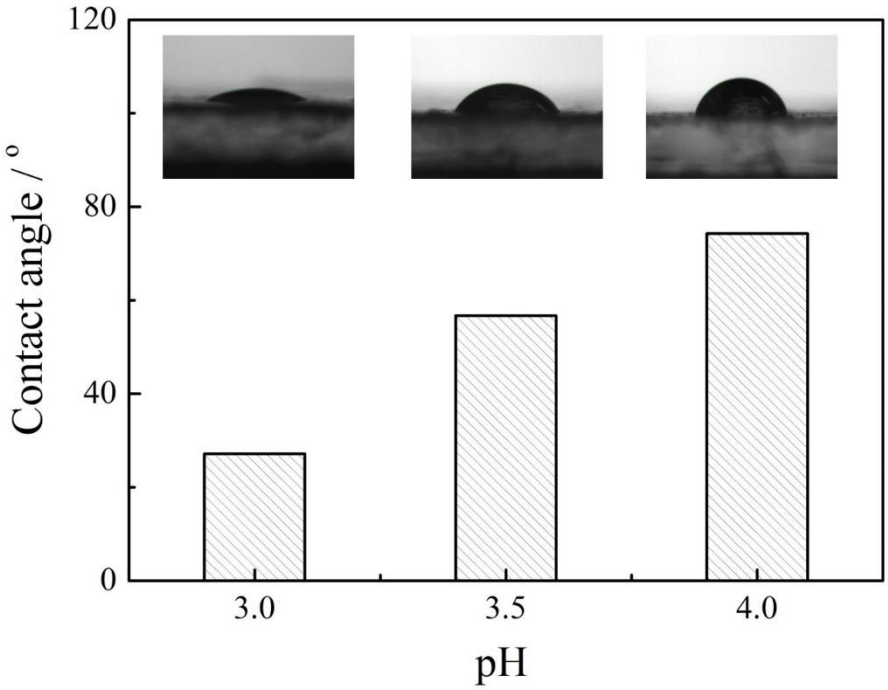

Fig.5 The wettability of (CSn/PAA2.8)*30 (n=4.0, 3.5 and 3.0 respectively) multilayer polyelectrolyte films

The dynamic self-healing processes of the (CSn/PAA2.8)*30 multilayer polyelectrolyte self-healing films were observed via stereomicroscope. Firstly, the films were cut with a scalpel. The cut width was about 30 μm, which penetrated to the subtrate's surface. Fig 6 (a), (e), and (i) are the results of multilayer polyelectrolyte self-healing films after injury treatment. When a drop of ultra-pure water is injected into the film via a syringe, the film expands rapidly after absorbing the water, and scratch disappears quickly. Meanwhile, the damaged part without stimulation via water experiences no change in volume and cannot heal itself (j). Then, as the water slowly expands the film, the damaged part repairs itself constantly (k). Finally, when the film is completely infiltrated by the water, the scratch disappears. The damaged part cannot be found. Thus, the film heals itself completely (l). In the control experiment, the damaged part of the (CS3.5/PAA2.8)*30 film also expands after absorbing the water (f), but the cut does not disappear (g), even after immersing the film in water for 10 min, it cannot accomplish the self-healing process successfully

(h); moreover, the damaged part of the (CS4.0/PAA2.8)*30 film has little response to water in terms of volume change and fails to repair itself (a—d).

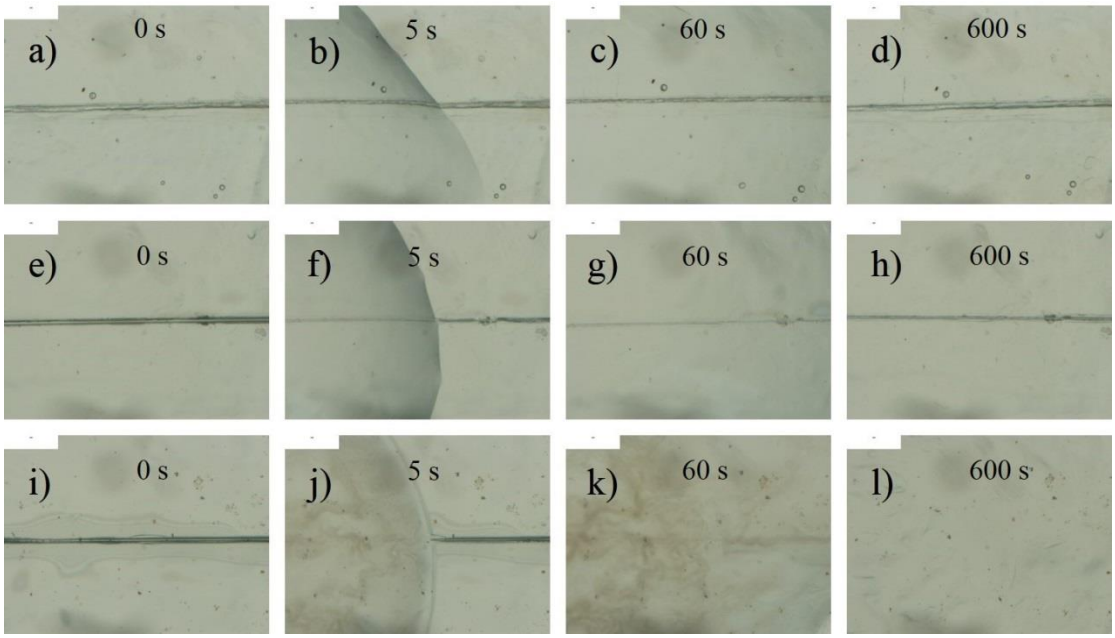

Fig. 6 The self-healing process of (CS4.0/PAA2.8)*30 (a-d), (CS3.5/PAA2.8)*30 (e-h) and (CS3.0/PAA2.8)*30 (i-l)) multilayer polyelectrolyte films, respectively. The scale bar is 300 μm.

Based on the self-healing phenomena observed above, one can speculate regarding the self-healing mechanism of the prepared multilayer polyelectrolyte film, as seen in Fig. 7: (I) Multilayer polyelectrolyte self-healing film presents a flat surface; (II) after the damage treatment, the functional groups remain dissociated across the damaged zone; (III) after stimulation (water), the film can mobilize to a certain extent via expanding in volume rapidly, lending the site of injury a certain fluidity. Thus, the damaged zone can contact one another. Meanwhile, stimulated by the water, the original interactions (hydrogen bonds) of the film become weak, so the damaged zones can interact with each other; (IV) when the water is removed from the film, the hydrogen bonds regenerate immediately, and the film completes the self-healing process.

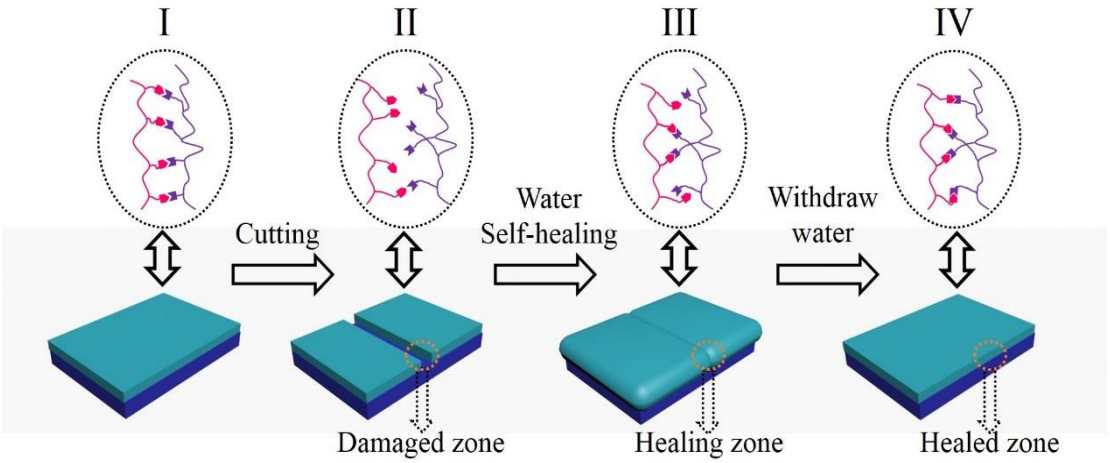

Fig.7 Schematic illustration of self-healing mechanism of self-healing multilayer polyelectrolyte film.

Generally, partly because the covalent bond of the polymer chains have little free carries (electrons) and the polymer molecules pile together due to van der Waals forces, electron overlap between the molecules is poor, so the free carries are very difficult to mobilize in the polymer, causing to the electrical conductivity of the polymer to be poor. Thus, the prepared polymer electrodes have poor conductivity, while the substrate, ITO glass, has good conductivity. If the polymer film is damaged and cannot heal itself immediately, the ITO will be exposed to the electrolyte solution, and the resistance of the electrode will be reduced; if the damaged polymer film can repair itself, the exposed ITO will re-cover the polymer, and the resistance will not change very much. Thus, by comparing the original resistance with that after the cut and self-healing, the self-healing process can be evaluated. Wei Wang and co-workers also used electrochemical impedance spectroscopy (EIS) to monitor the self-healing process.[47] Inspired by this, EIS was used to further confirm the self-healing properties of the damaged (CSn/PAA2.8)*30 coatings, Fig 8 presents the Nyquist plots of the (CSn/PAA2.8)*30 multilayer polyelectrolyte film electrodes at a steady state after being activated. It can be seen that the Nyquist plots of the three electrodes display a slope in the low-frequency region and a depressed semicircle resulting from charge-transfer resistance in the high-frequency region.[48] Moreover, the detailed numerical result of the charge-transfer resistance is presented in Fig 8. The charge-transfer resistance of the original (CS4.0/PAA2.8)*30 multilayer

polyelectrolyte film electrode is 1,206 Ω. After injury treatment (the cut width is about 30 μm) and then immersing the electrode in water for 10 min, the charge-transfer resistance of the (CS4.0/PAA2.8)*30 changes to 409.3Ω, which indicates that it cannot heal itself. The original (CS3.5/PAA2.8)*30 multilayer polyelectrolyte film electrode is 993.4 Ω; after the cut and self-healing process, the charge-transfer resistance of the (CS3.5/PAA2.8)*30 changed to 518.2Ω. It also cannot repair itself completely. The original (CS3.0/PAA2.8)*30 multilayer polyelectrolyte film electrode is 826 Ω. After the cut and self-healing process, the resistance changed a little (to 809 Ω), indicating that the (CS3.0/PAA2.8)*30 multilayer polyelectrolyte film can heal itself. The results are consistent with the earlier findings obtained via optical microscope.

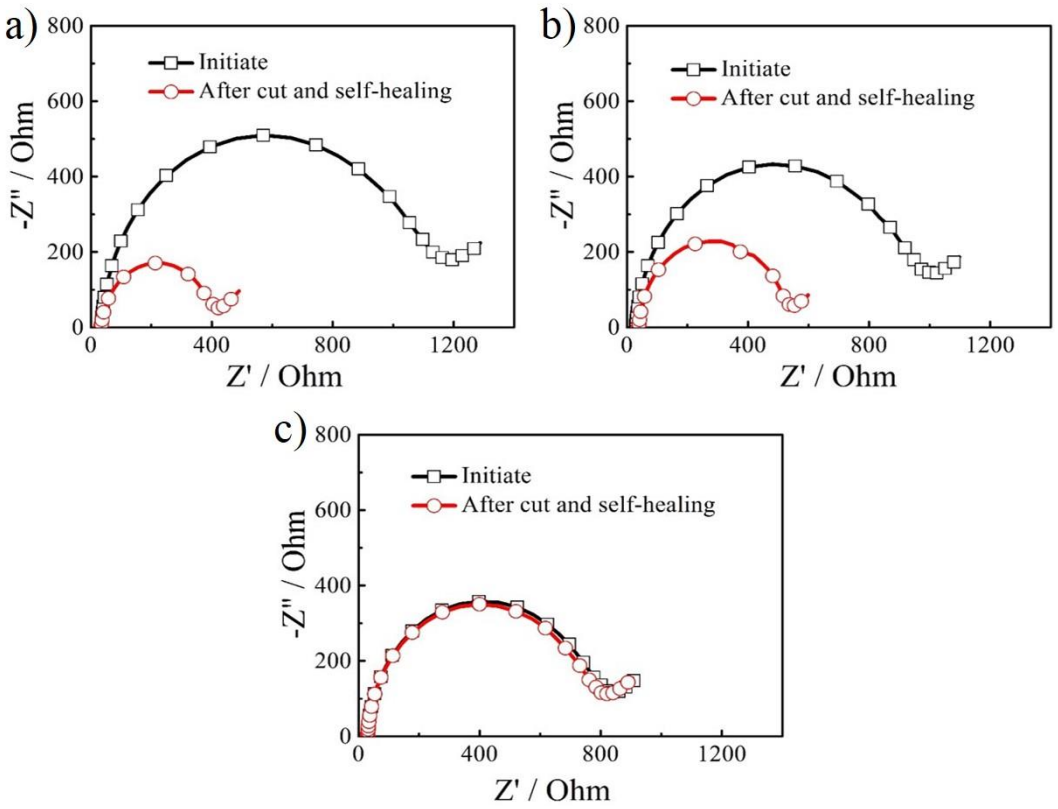

Fig. 8 The Nyquist plots of (CSn/PAA2.8)*30 (n=4.0 (a), 3.5 (b) and 3.0 (c) respectively) multilayer polyelectrolyte films

4. Conclusions

In summary, an environmentally friendly, facile, and simple method of synthesizing CS/PAA multilayer polyelectrolyte film was developed. First, the specific structural

parameters of the various hydrogen bonds were calculated. Then, multilayer polyelectrolyte films were fabricated with CS and PAA based on LbL self-assembling technology at different pH values. The possible influence of pH on the preparation mechanism, compositions, microstructure, wettability, and self-healing ability of the (CSn/PAA2.8)*30 multilayer polyelectrolyte films were investigated. The results show that the interactions between CS and PAA, swelling capacity, wettability, and self-healing ability are all governed by the pH of the CS solution. When the pH value is 4.0, the prepared multilayer polyelectrolyte film, (CS4.0/PAA2.8)*30, has little response to water in terms of changing its volume and thus cannot heal itself. Although the (CS3.5/PAA2.8)*30 multilayer polyelectrolyte film can expand after absorbing the water, the damaged zones cannot interact with each other. Thus, it also fails to accomplish the self-healing process successfully. However, the prepared (CS3.0/PAA2.8)*30 multilayer polyelectrolyte film can repair itself via volume expansion and interactions between the damaged zones quickly. It shows excellent self-healing ability in a water environment. Given that CS can be readily engineered and functionalized with the desired properties and be easily assembled on the multilayer polyelectrolyte film, via this method, different types of functional self-healing films can be fabricated. This will have practical applications in various devices due to enhanced durability and reliability.

Acknowledgments

The authors thank for the financial support of pre-research foundation for national science foundation and the Fundamental Research Funds for the Central Universities. Y. Zhu thanks for the support the fund for the analysis and testing of the large-scale apparatus and the Scientific Research Foundation of Graduate School of Southeast University. Prof. Dr. Ge also thanks for the support from Prof. Dr. Guzhongze's group.

References

1. M. D. Hager, P. Greil, C. Leyens, S. van der Zwaag and U. S. Schubert, *Adv. Mater.*, 2010, **22**, 5424-5430.
2. D. Sun, J. An, G. Wu and J. Yang, J. Mater. Chem. A, 2015, **3**, 4435-4444.
3. D. Y. Wu, S. Meure and D. Solomon, *Prog. Polym. Sci.*, 2008, **33**, 479-522.

4. P. Cordier, F. Tournilhac, C. Souli é-Ziakovic and L. Leibler, *Nature*, 2008, **451**, 977-980.
5. Y. Amamoto, J. Kamada, H. Otsuka, A. Takahara and K. Matyjaszewski, *Angew. Chem. Int. Ed.*, 2011, **123**, 1698-1701.
6. H. Zhang, D. Han, Q. Yan, D. Fortin, H. Xia and Y. Zhao, *J. Mater. Chem. A*, 2014, **2**, 13373-13379.
7. J. A. Syrett, C. R. Becer and D. M. Haddleton, *Polym. Chem.*, 2010, **1**, 978-987.
8. Y. Chen, A. M. Kushner, G. A. Williams and Z. Guan, *Nature Chem.*, 2012, **4**, 467-472.
9. X. Wang, Y. Wang, S. Bi, Y. Wang, X. Chen, L. Qiu and J. Sun, *Adv. Funct. Mater.*, 2014, **24**, 403-411.
10. X. Wang, F. Liu, X. Zheng and J. Sun, *Angew. Chem. Int. Ed.*, 2011, **50**, 11378-11381.
11. Y. Chen and Z. Guan, *Chem. Commun.*, 2014, **50**, 10868-10870.
12. B. Blaiszik, S. Kramer, S. Olugebefola, J. S. Moore, N. R. Sottos and S. R. White, *Annu. Rev. Mater. Res.*, 2010, **40**, 179-211.
13. L. Zhang, J. Wu, N. Sun, X. Zhang and L. Jiang, *J. Mater. Chem. A*, 2014, **2**, 7666-7668.
14. M. Zhang, D. Xu, X. Yan, J. Chen, S. Dong, B. Zheng and F. Huang, *Angew. Chem. Int. Ed.*, 2012, **124**, 7117-7121.
15. T. R. Cook, Y.-R. Zheng and P. J. Stang, *Chem. Rev.*, 2012, **113**, 734-777.
16. F. Herbst, D. Döhler, P. Michael and W. H. Binder, *Macromol. Rapid Commun.*, 2013, **34**, 203-220.
17. Z. Wei, J. H. Yang, Z. Q. Liu, F. Xu, J. X. Zhou, M. Zr ńyi, Y. Osada and Y. M. Chen, *Adv. Funct. Mater.*, 2015, **25**, 1352-1359.
18. Q. Chen, L. Zhu, H. Chen, H. Yan, L. Huang, J. Yang and J. Zheng, *Adv. Funct. Mater.*, 2015, **25**, 1598-1607.
19. Z. Wei, J. H. Yang, J. Zhou, F. Xu, M. Zr ńyi, P. H. Dussault, Y. Osada and Y. M. Chen, *Chem. Soc. Rev.*, 2014, **43**, 8114-8131.
20. P. Taynton, K. Yu, R. K. Shoemaker, Y. Jin, H. J. Qi and W. Zhang, *Adv. Mater.*, 2014, **26**, 3938-3942.
21. Y. Li, X. Wang and J. Sun, *Chem. Soc. Rev.*, 2012, **41**, 5998-6009.
22. E. V. Skorb and D. V. Andreeva, *Polym. Chem.*, 2013, **4**, 4834-4845.
23. Q. Han, C. Li, Y. Guan, X. Zhu and Y. Zhang, *Polymer*, 2014, **55**, 2197-2204.
24. Y. Li, S. Chen, M. Wu and J. Sun, *Adv. Mater.*, 2014, **26**, 3344-3348.
25. Y. Wang, T. Li, S. Li, R. Guo and J. Sun, *ACS Appl. Mater. Interfaces*, 2015, **7** 13597-13603.
26. A. B. South and L. A. Lyon, *Angew. Chem. Int. Ed.*, 2010, **122**, 779-783.
27. R. Merindol, S. Diabang, O. Felix, T. Roland, C. Gauthier and G. Decher, *ACS nano*, 2015, **9**, 1127-1136.
28. Y. Gu and N. S. Zacharia, *Adv. Funct. Mater.*, 2015.**25**, 3785–3792.
29. Y. Zhu, C. Yao, J. Ren, C. Liu and L. Ge, *Colloids Surf., A*, 2015, **465**, 26-31.
30. S. C. Chen, Y. C. Wu, F. L. Mi, Y. H. Lin, L. C. Yu and H. W. Sung, *J.*

Controlled Release, 2004, **96**, 285-300.
31. Y. Zhang, L. Tao, S. Li and Y. Wei, *Biomacromolecules*, 2011, **12**, 2894-2901.
32. L. Sun, L. Zhang, C. Liang, Z. Yuan, Y. Zhang, W. Xu, J. Zhang and Y. Chen, *J. Mater. Chem.*, 2011, **21**, 5877-5880.
33. S. Yang, J. Li, D. Shao, J. Hu and X. Wang, *J. Hazard. Mater.*, 2009, **166**, 109-116.
34. Z. Li, Y. Li, Z. Cao, J. Gu, K. Liu, W. Zhao and X. Wang, *Med. Chem. Res.*, 2014, **23**, 3916-3926.
35. D. Pan, J. Cao, H. Guo and B. Zhao, *Food Chem.*, 2012, **130**, 121-126.
36. M. Frisch, G. Trucks, H. Schlegal, G. Scuseria, M. Robb, J. Cheesman, V. Zakrzewski, J. Montgomery Jr, R. Stratmann and J. Burant, *Gaussian Inc., Pittsburgh, PA*, 2009.
37. A. D. Becke, *J. Chem. Phys.*, 1993, **98**, 5648-5652.
38. M. Cossi, V. Barone, R. Cammi and J. Tomasi, *Chem. Phys. Lett.*, 1996, **255**, 327-335.
38. M. Labib, M. Hedström, M. Amin and B. Mattiasson, *Anal. Chim. Acta*, 2009, **634**, 255-261.
39. J. Choi and M. F. Rubner, *Macromolecules*, 2005, **38**, 116-124.
40. K. Itano, J. Choi and M. F. Rubner, *Macromolecules*, 2005, **38**, 3450-3460.
41. Y. Hu, X. Jiang, Y. Ding, H. Ge, Y. Yuan and C. Yang, *Biomaterials*, 2002, **23**, 3193-3201.
42. C. Hu, B. Li, R. Guo, H. Wu and Z. Jiang, *Sep. Purif. Technol.*, 2007, **55**, 327-334.
43. P. Lavalle, C. Picart, J. Mutterer, C. Gergely, H. Reiss, J. C. Voegel, B. Senger and P. Schaaf, *J. Phys. Chem. B*, 2004, **108**, 635-648.
44. Y. Zhao, H. Su, L. Fang and T. Tan, *Polymer*, 2005, **46**, 5368-5376.
45. R. P. Wool, *Adv. Mater.*, 2008, **4**, 400-418.
46. M. Padaki, A. M. Isloor, J. Fernandes and K. N. Prabhu, *Desalination*, 2011, **280**, 419-423.
47. W. Wang, L. Xu, X. Li, Z. Lin, Y. Yang and E. An, *J. Mater. Chem. A*, 2014, **2**, 1914-1921.
48. Y. Li, J. Yao, Y. Zhu, Z. Zou and H. Wang, *J. Power Sources*, 2012, **203**, 177-183.